06/07 NOVIEMBRE

IPG 2025
INTERNATIONAL PIPELINE GEOTECHNICAL CONFERENCE

Organizan:
CIPG COMITÉ TÉCNICO
ACIEM Asociación Colombiana de Ingenieros

Aprovechamiento de Imágenes Satelitales y Modelos Geoespaciales para el Monitoreo de Cruces de Ríos

GeoHAS

Vanessa Cuervo, Daniel Cuervo, Yarelis Gutiérrez,
Gabriela Omaña, Gio Roberti, Luis Aguiar

07 de Noviembre de 2025

Esquema de la presentación

01

Introducción

- Retos del monitoreo en cruces de rio
- Propuesta de monitoreo en marco GeoHAS

02

Metodología

- Fuentes de datos
- Áreas de estudio
- Enfoque metodológico

03

Resultados y Discusión

- Resumen por áreas
- Validación y eficiencia
- Limitaciones y desarrollos próximos

Andes Geo

Amenazas a la integridad

1. **Los cruces de ríos son sistemas dinámicos**
2. **Los procesos fluviales de migración de cauces y erosión de bancos comprometen tuberías**
3. **El riesgo está asociado a la exposición (interacción)**
4. **Los esfuerzos de mitigación son costosos**

Andes Geo

01- Introducción

- Las inspecciones de campo demandan tiempo y recursos
- Difíciles de realizar en lugares remotos

02- Metodología

¿Qué es GeoHAS?

GeoHAS

Algoritmos impulsados por IA

Aplicación web y móvil

API escalable

Equipo de especialistas

Andes Geo

02- Metodología

1. Imágenes satelitales (múltiples sensores)
2. Google Earth Engine
3. Paquete samgeo (Python +SAM)
4. Detección y cuantificación

Andes Geo

Fuentes de datos

- Misión multiespectral de ESA
- 13 bandas espectrales (443-2,190 nm)
- Resolución espacial: 10m, 20m, 60m
- Tiempo de revisita: 5 días en el ecuador
- Datos gratuitos (Level-1C y Level-2A)
- 2019-2024

Sentinel-2/Landsat

- Imágenes satelitales y aéreas de alta resolución
- Disponible desde febrero 2014
- Basemap World Imagery en ArcGIS Living Atlas

Múltiples sensores

Esri, World Imagery Wayback{/nav}} (version date: 2025-05-29).
[Link: Wayback Archive link
https://https://livingatlas.arcgis.com/wayback/#mapCenter=-75.16393%2C-9.90097%2C14&mode=explore&active=25285

Andes Geo

Áreas de prueba

Área 1: Río Tumbes (Costa)
- Patrón meándrico
- Afectado por eventos ENSO

Área 2: Río Santa (Costa)
- Patrón anastomosado
- Baja pendiente, inestabilidad lateral

Área 3: Río Huallaga (Amazonía)
- Afluente del Marañón
- Migración lateral, lagos oxbow

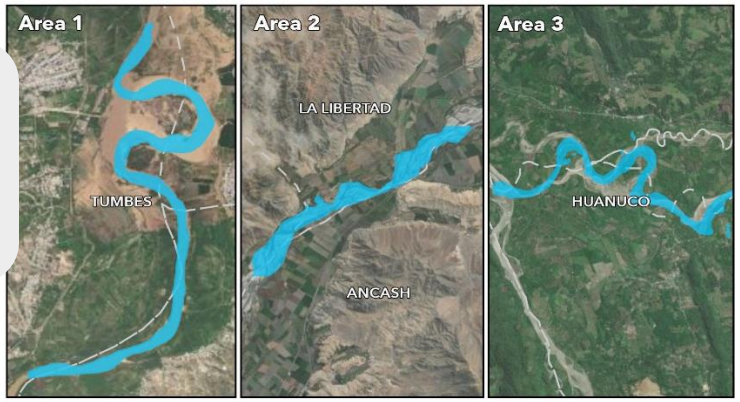

Andes Geo

Monitoreo de series temporales

- Mosaicos Sentinel-2 sin nubes (2019-2024).
- Cálculo de índices espectrales (MNDWI + NDBI).
- Extracción de la geometría de canal activo.
- Análisis anual de cambios.

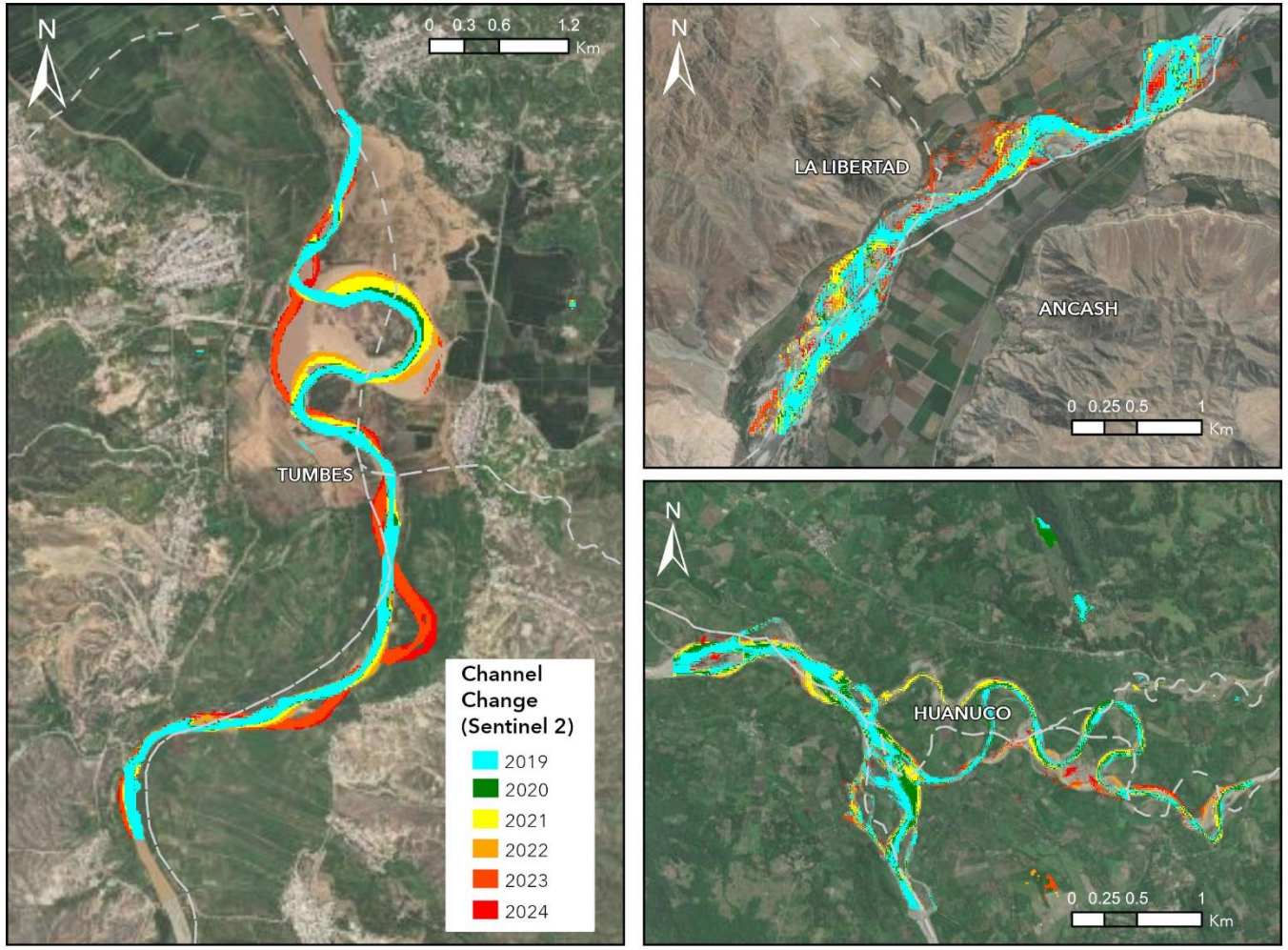

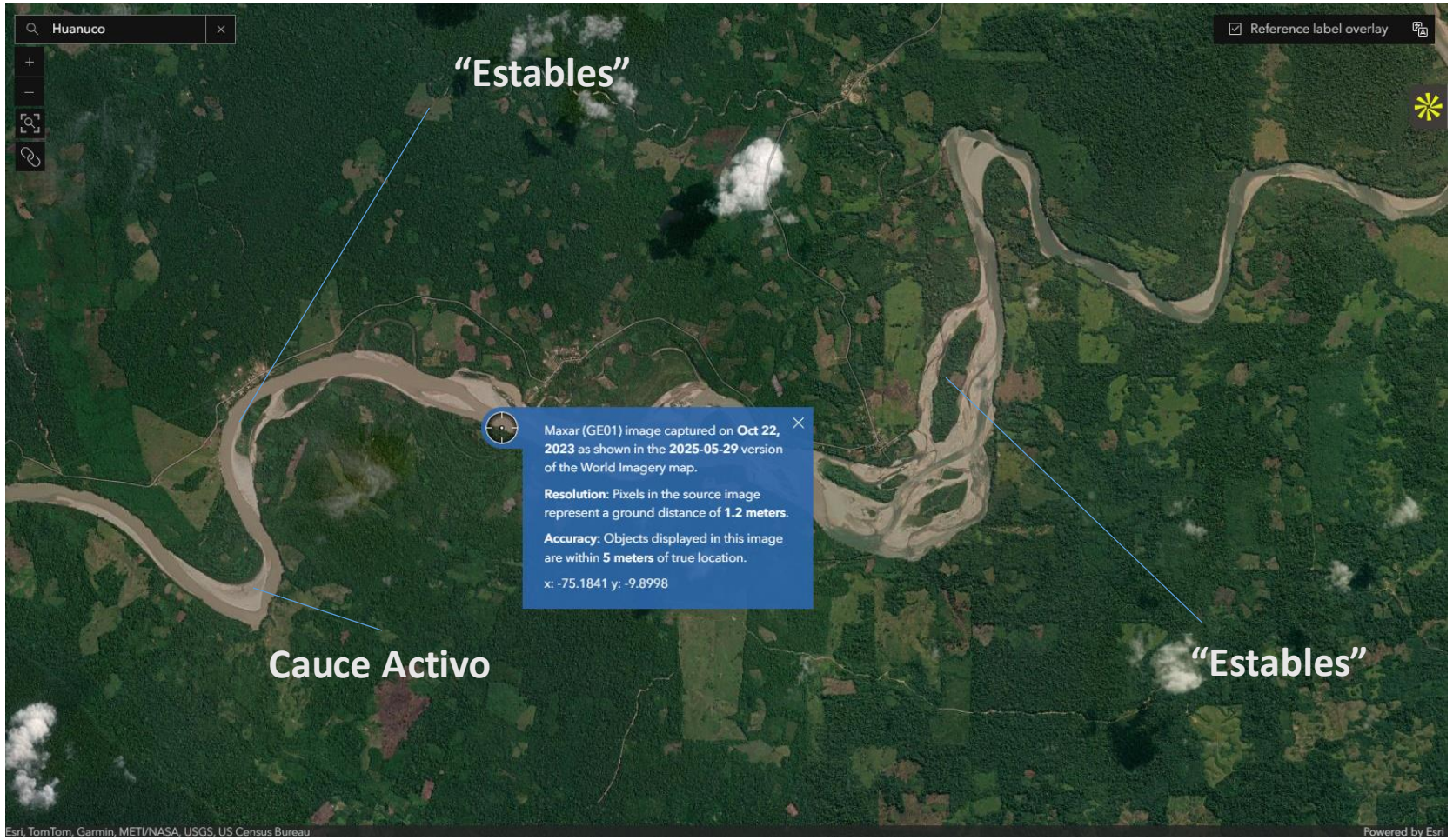

Mapeo de cauce activo

Andes Geo

02- Metodología

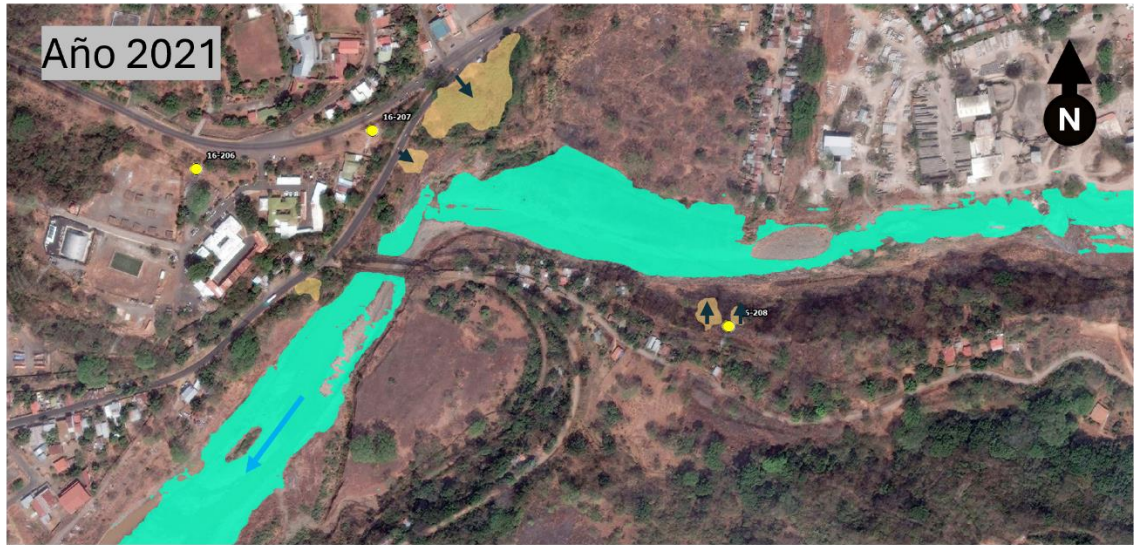

Fuente: Andes Geo – GeoHAS (2025). Channel Mapper Documentation.

Cambios en cauce activo

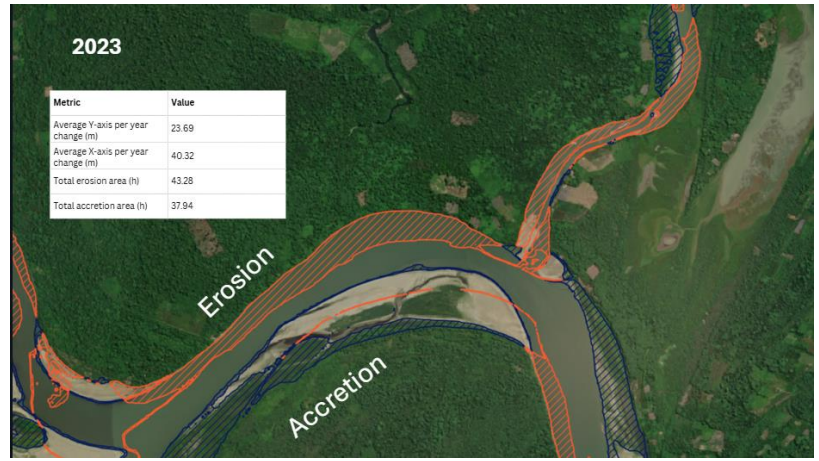

Fuente: Andes Geo – GeoHAS (2025). Channel Mapper Documentation.

Índice de riesgo

$$RI = w1 \times (\Delta C/\Delta t) + w2 \times T + w3 \times E\_max + w4 \times (W/D\_inf)$$

RI = Índice de Riesgo (adimensional)
(ΔC/Δt) = Tasa de cambio del canal dentro del tramo (m/año o m/tiempo)
T = Factor de tendencia (parámetro adimensional que cuantifica patrones de cambio gradual vs. súbito)
E_max = Erosión máxima en el sitio del cruce (m)
W = Ancho del canal (m)
D_inf = Distancia desde la infraestructura al elemento en riesgo (m)
D_cover = Profundidad mínima de recubrimiento para infraestructura enterrada (m)
w_1, w_2, w_3, w_4, w_5 = Coeficientes de ponderación (adimensionales, $\Sigma w_i = 1$)

Fuente: Andes Geo – GeoHAS (2025). Channel Mapper Documentation.

Andes Geo

02- Resultados y Discusión

Área 1: Tumbes (Costa)

- Sistema altamente activo dominado por migración lateral
- Cambios abruptos entre 2023-2024
- Erosión de márgenes significativa
- Característica típica de ríos de alta sinuosidad en llanuras aluviales

Erosión promedio en Y
28,9 m

Erosión promedio en promedio en X
35,3 m

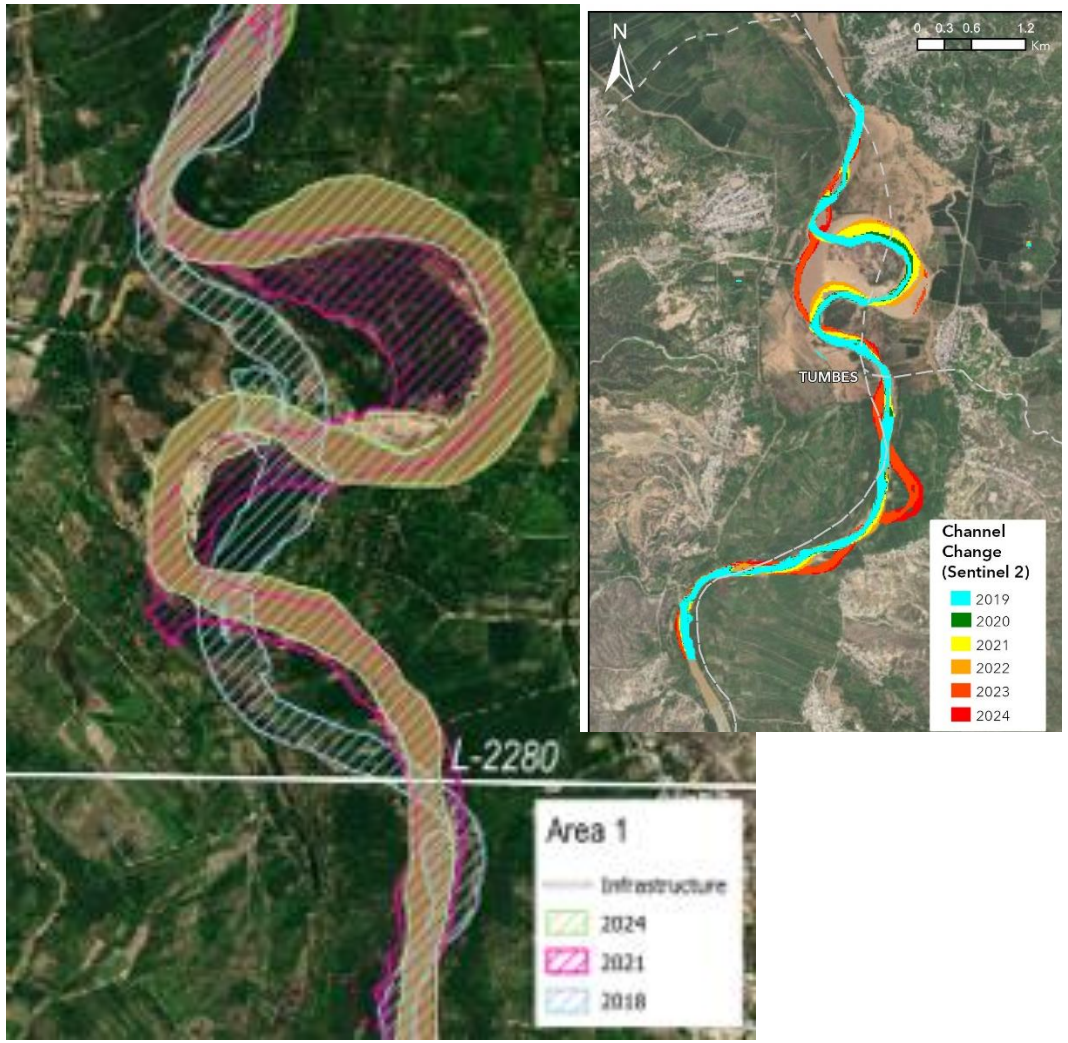

Andes Geo

02- Resultados y Discusión

Erosión promedio en Y
18,6 m

Erosión promedio en promedio en X
29,0 m

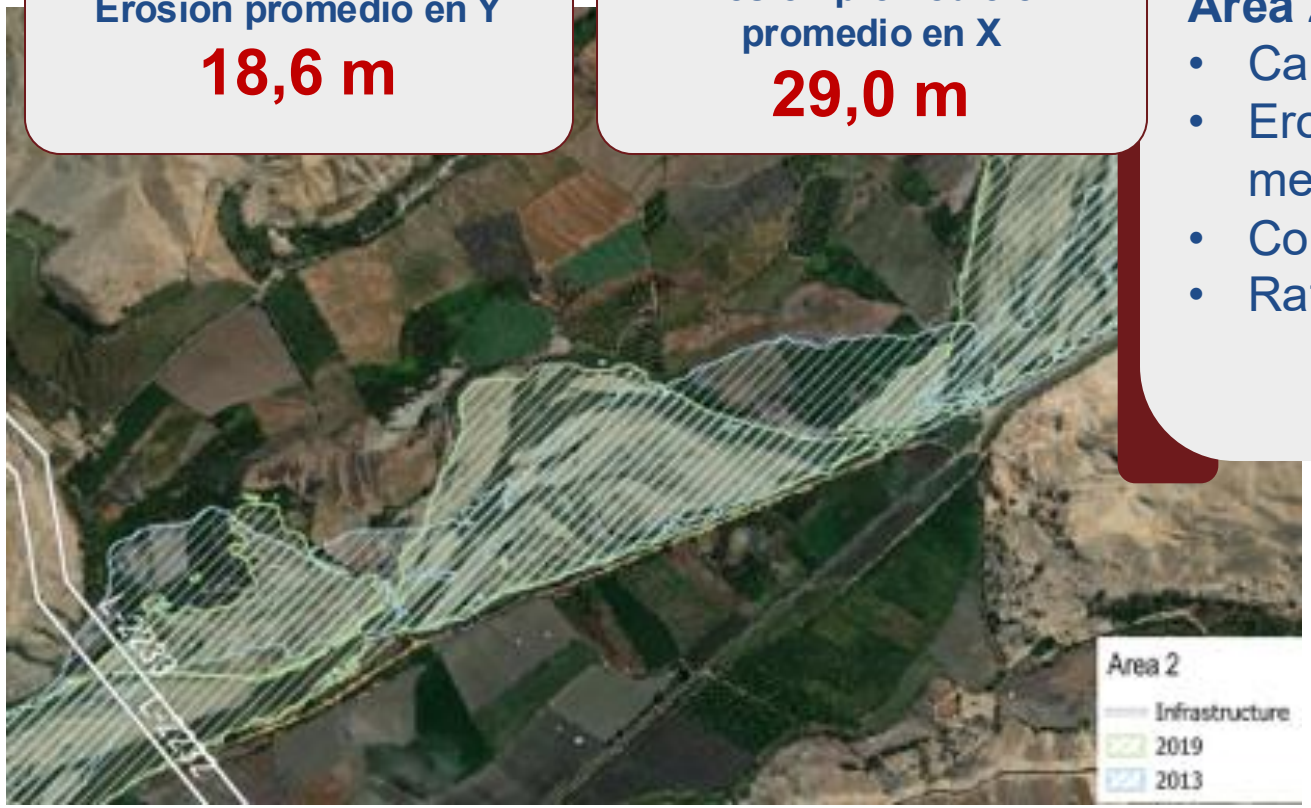

Área 2: Río Santa (Costa)

- Cambios dentro de llanura aluvial activa
- Erosión significativa en curvas externas de meandros
- Consistente con morfología anastomosada
- Ratios erosión/acreción más balanceados

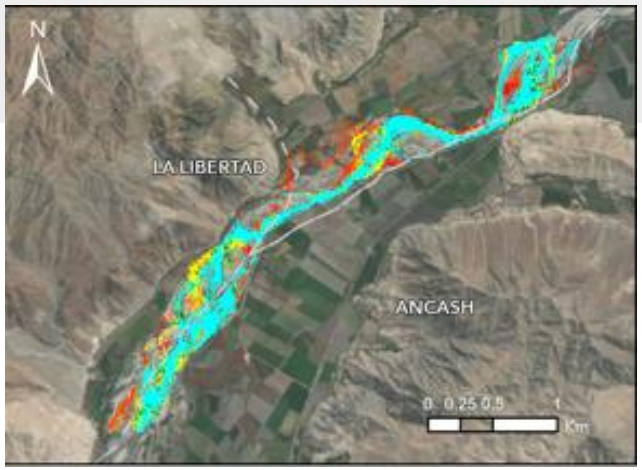

Andes Geo

02- Resultados y Discusión

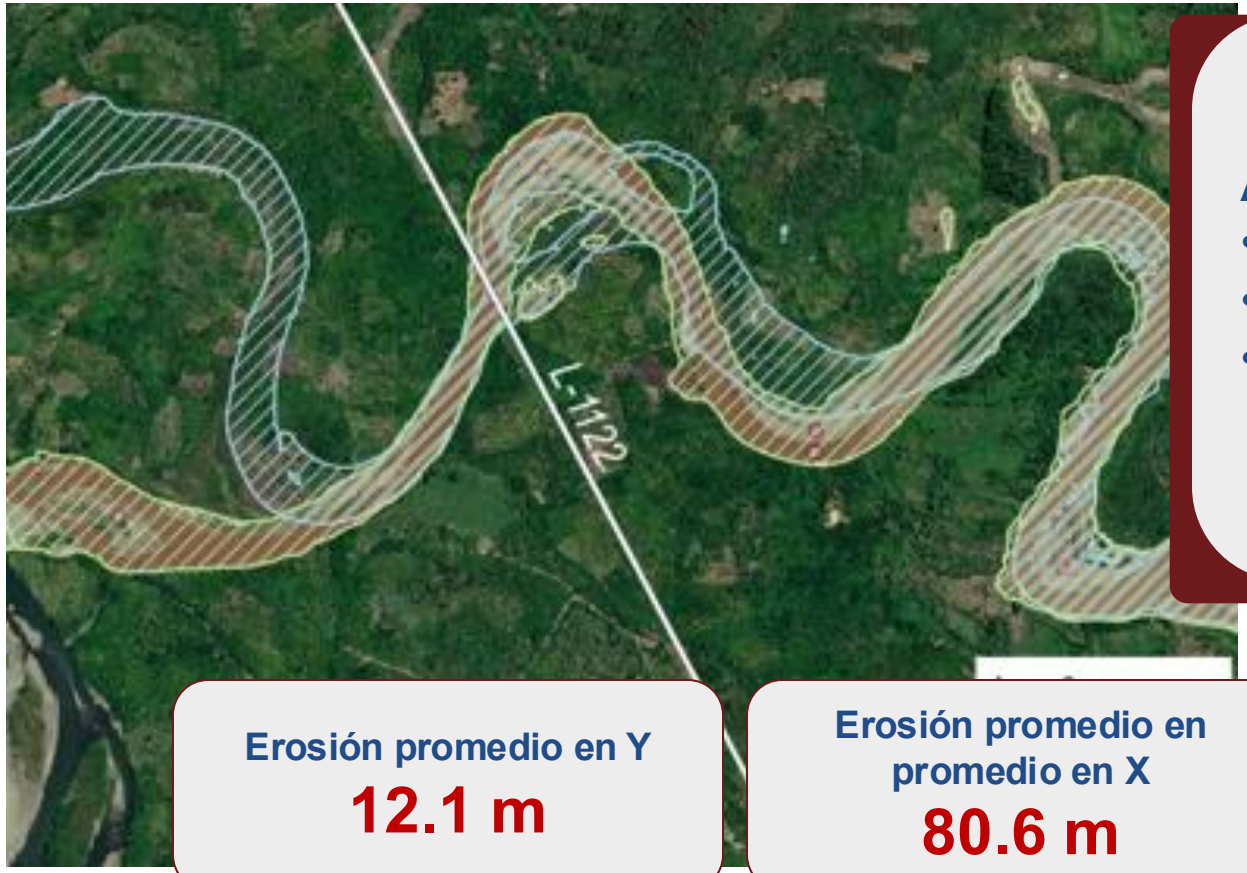

Erosión promedio en Y
12.1 m

Erosión promedio en promedio en X
80.6 m

Área 3: Río Huallaga (Amazonía)

- Cambios súbitos en el período analizado
- Dinámica activa típica de ríos sinuosos
- Llanuras aluviales amplias

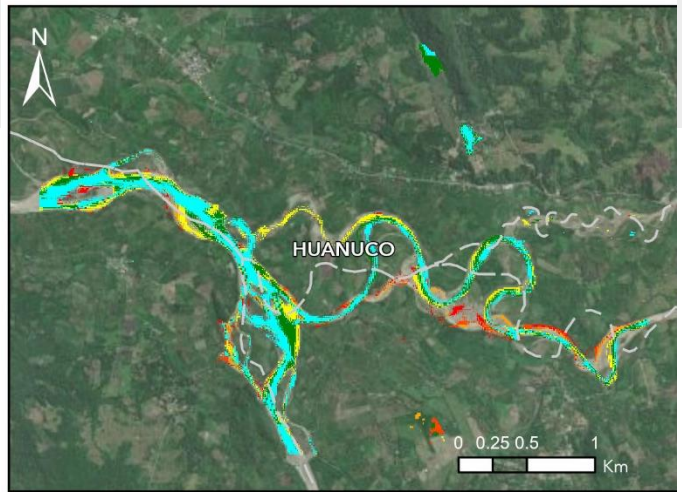

Andes Geo

02- Resultados y Discusión

Esfuerzo manual: 6,0 horas totales (≈2,0 horas/ubicación)
Esfuerzo automatizado: 9 minutos (≈3 minutos/ubicación)
Ganancia de eficiencia: 40× más rápido → de 0,5 ubicaciones/hora a 20 ubicaciones/hora

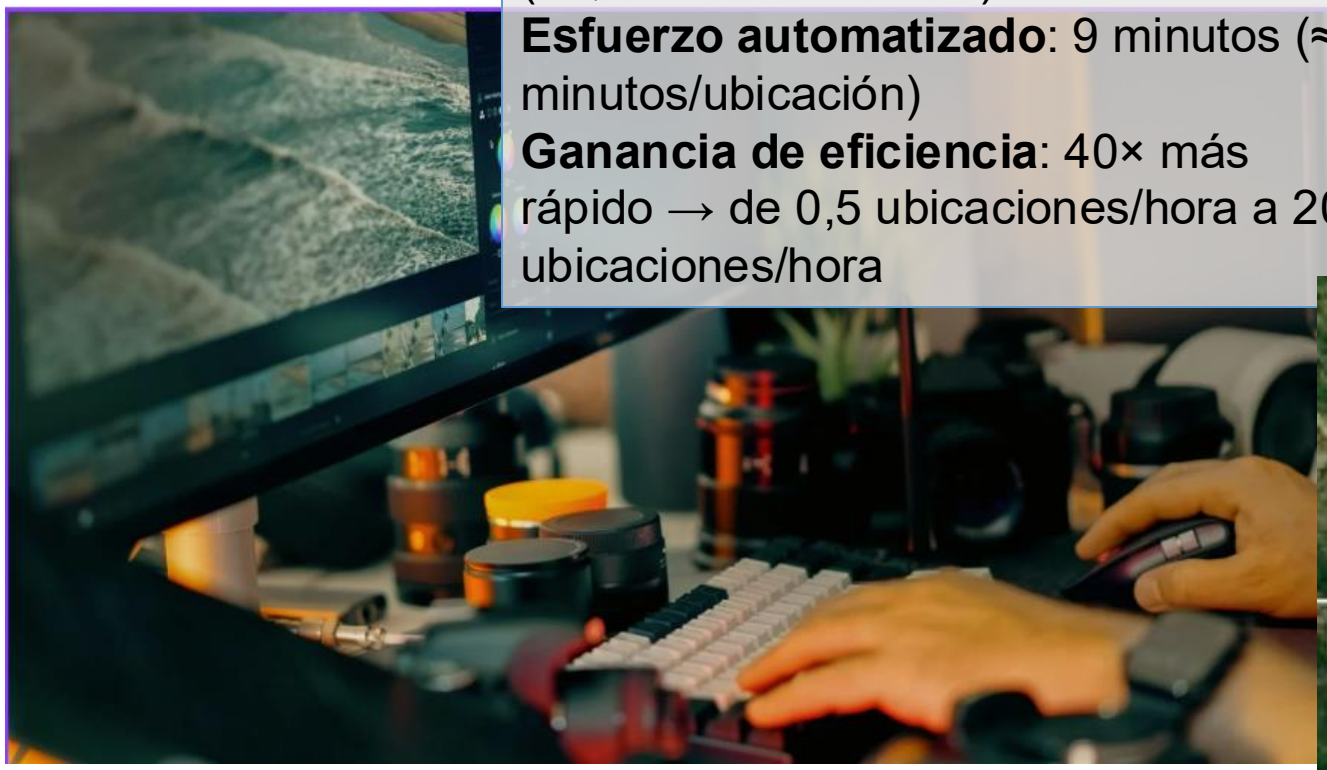

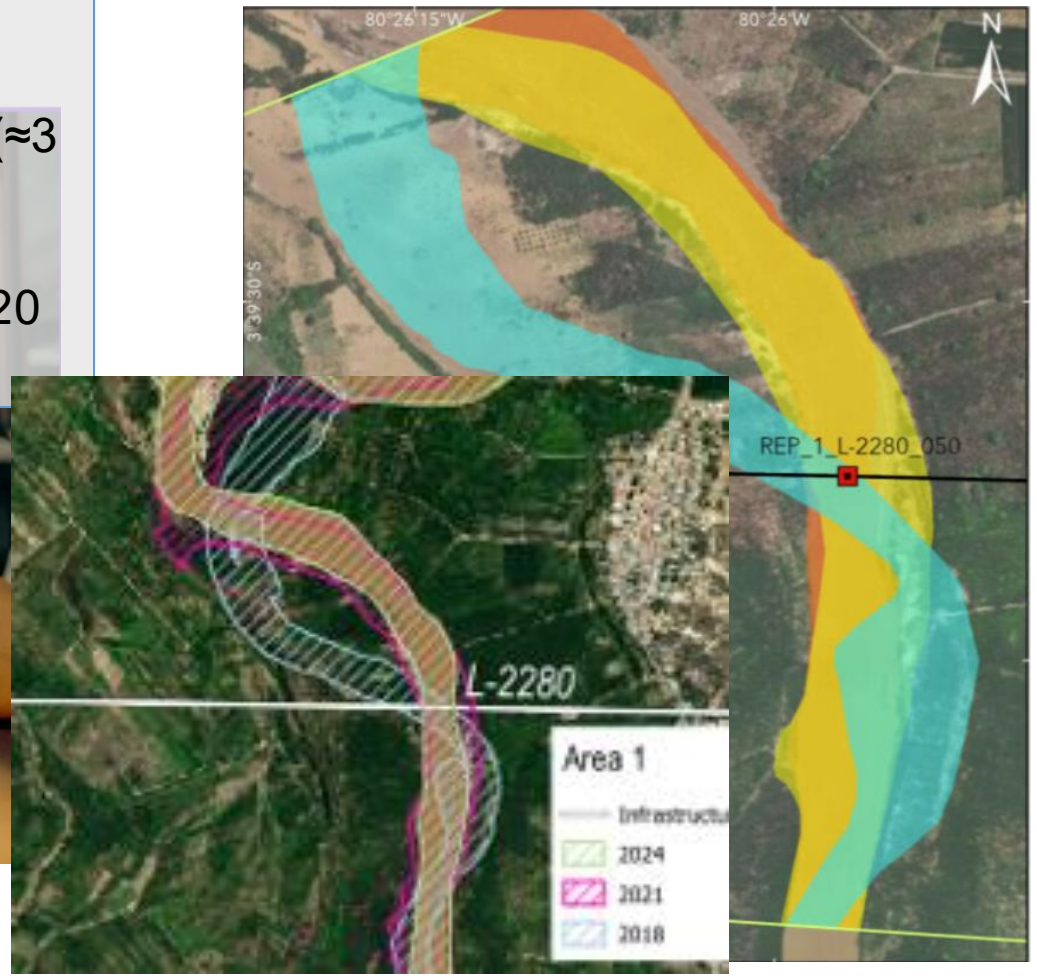

Andes Geo

02- Resultados y Discusión

- La definición de secciones homogéneas y puntos semillas **requiere de un analista –** se plantea implementar criterios basados en elevación
- **Variabilidad estacional del nivel del agua** – se plantea integrar datos hidrológicos para contextualizar cambios
- **Límite de resolución** (Sentinel-2): el análisis se restringe a ríos de ≥10 m de ancho - ríos más pequeños requerirán adquisiciones más frecuentes de alta resolución
- **Análisis de escritorio –** todo monitoreo requiere datos de campo para optimizar la estimación de coeficientes. Visitas de validación/calibración.

Andes Geo

Conclusiones

1. **Desplazamiento lateral**
   Decenas de metros/año en morfologías meándricas anastomosadas

2. **Índice de riesgo ponderado**
   Permite priorizar inspecciones, mantenimiento y preparación de emergencias.

3. **Reducción de costos**
   Datos de bajo costo + procesamiento en la nube = accesible para organizaciones con recursos limitados

4. **Eficiencia**
   Mejora 40x vs. métodos manuales

5. **Posibilidad de cuantificación**

   En el orden de metros con el uso de imágenes satelitales

6. **Herramienta proactiva**

   Posibilidad de monitoreo más frecuente en un clima cambiante

Andes Geo

Gracias

Vanessa Cuervo, M.Sc.
CEO, Principal Hazard and Risk Specialist

Email: vcuervo@andes-geo.com


¡Gracias!

IPG 2025 7th International Pipeline Geotechnical Conference
IPG2025
6-7 November 2025, Bogota, Colombia

IPG2025-016

LEVERAGING SATELLITE IMAGERY AND GEOSPATIAL MODELS TO MONITOR PIPELINE WATER CROSSINGS

Vanessa Cuervo
Andes Geo
Calgary, Canada

Daniel Cuervo
Andes Geo
Santiago, Chile

Yarelis Gutiérrez
Andes Geo
Santiago, Chile

Gabriela Omaña
Andes Geo
Calgary, Canada

Gio Roberti
Andes Geo
Squamish, Canada

Luis Aguiar
Andes Geo
Calgary, Canada

ABSTRACT

Rivers are dynamic systems shaped by natural processes and human activities, which can significantly impact their morphology and behavior. Pipelines cross many rivers and stream channels. Fluvial processes, such as channel migration and bank erosion, pose significant risks to pipeline integrity, potentially leading to pipeline exposure and right-of-way (ROW) encroachment, resulting in costly mitigation efforts. Field-based inspections of each crossing are time-consuming and resource-intensive, particularly across remote or inaccessible terrain. To overcome this challenge, we present an automated, scalable methodology that leverages satellite imagery and cloud-based geospatial analysis to detect and quantify planform changes at pipeline river crossings.

Our approach, which is part of the GeoHAS (Geospatial Hazard Assessment Solution), combines high-resolution imagery from various sensors with Google Earth Engine and the Python-based samgeo package to map active river channels, define bank positions, and identify changes in vegetation that indicate geomorphic activity. This method estimates average shifts in bank positions over time and highlights areas of potential concern for pipeline operators. By automating the traditional manual process of detecting channel shifts, our method reduces assessment times from days to minutes while maintaining spatial accuracy within the order of centimeters (provided that the imagery is captured under similar flow conditions). This work provides advantages for geohazard specialists and stakeholders involved in pipeline and infrastructure management. It enables proactive decision-making for maintenance planning, emergency response, and route optimization, which ultimately enhances the safety and resilience of pipeline systems.

Keywords: Channel change, bank erosion, pipeline water crossings, satellite imagery, sam-geo, Level Two assessment.

NOMENCLATURE

ENSO	El Niño–Southern Oscillation
GEE	Google Earth Engine
GeoHAS	Geospatial Hazard Assessment Solution
MNDWI	Modified Normalized Difference Water Index
SAM	Segment Anything Model

1. INTRODUCTION

Pipeline infrastructure frequently crosses fluvial systems, where dynamic riverine processes such as channel migration and bank erosion pose hydrotechnical hazards. These morphodynamic processes, driven by hydrologic variability, sediment transport, and watershed alterations, can modify channel planforms, destabilize banks, and result in substantial geomorphic changes over short timescales. For pipeline operators, such dynamics introduce critical threats to pipeline integrity, including potential exposure, loss of cover, and mechanical damage, particularly where channel movement intersects the right-of-way (ROW) [1, 2]. Historical and recent cases illustrate the severity of these risks. For example, Pembina Pipeline Corporation documented multiple instances of bank erosion and lateral channel migration threatening pipeline integrity across its 10,000 km network in Canada. Their geohazard program emphasizes proactive monitoring to mitigate rupture risks at high-consequence crossings [3]. Channel incision and lateral erosion often lead to failures at pipeline crossings, requiring costly remediation strategies such as bank stabilization and realignment [4]. Cumulative effective stream power shows a strong correlation with erosional hotspots along pipeline corridors, emphasizing the importance of spatially explicit and process-based monitoring frameworks [5]. Monitoring channel migration through traditional methods—

such as field surveys, aerial photogrammetry, and repeat cross-section analysis—demands significant data collection efforts, incurs high costs, and poses logistical challenges in remote or inaccessible areas. These techniques typically require seasonal or annual field campaigns, expose personnel to physical hazards, and suffer from limited temporal frequency, making them unsuitable for rapid response or system-wide risk surveillance [6, 7, 8, 9, 10]. While photogrammetric and UAV-based Structure-from-Motion methods offer high spatial resolution, they are constrained by weather conditions, access limitations, and the need for repeated observations to capture infrequent but geomorphically significant events [9, 11].

Recent advances in satellite remote sensing and cloud-based geospatial analysis have opened new opportunities for scalable monitoring of fluvial processes. Moderate to high-resolution imagery, available through platforms such as Google Earth Engine and SkySat, enables frequent and historical assessments of river morphology at low cost. The advent of machine learning models such as the Segment Anything Model (SAM) and geospatial wrappers like samgeo [12] allows for object-aware segmentation of river features, reducing the need for manual digitization and supporting near real-time detection of geomorphic changes. Integrated into cloud computing environments, these tools facilitate the development of automated, reproducible, and spatially explicit channel mapping methodologies [13, 14].

This paper presents a streamlined approach to assess channel change and evaluate its implications for pipeline water crossings. Our methodology, developed within the GeoHAS (Geospatial Hazard Assessment Solution) platform, integrates SAM-based segmentation with satellite imagery to detect channel planform evolution and quantify rates of lateral migration and bank displacement. We apply this framework to three riverine environments in Peru, representing a range of fluvial dynamics and climatic forcings, including ENSO-affected coastal deltas and highly mobile Amazonian rivers [15, 16]. The objectives of this study are threefold:

(1) To demonstrate a fast, automated approach for mapping active river channels using high-resolution satellite imagery and samgeo.

(2) To estimate spatially distributed rates of change in channel boundaries using a grid-based analysis framework.

(3) To evaluate the applicability of this workflow for identifying pipeline crossings potentially threatened by fluvial hazards and guiding risk mitigation strategies. By leveraging emerging technologies in Earth observation and artificial intelligence, this work contributes to advancing pipeline geohazard monitoring practices. It supports the transition toward proactive, data-driven asset management in fluvial environments.

2. METHODS

2.1 Data

2.1.1 ESRI Wayback Imagery

Esri's World Imagery Wayback is an interactive collection of high-resolution satellite and aerial orthoimages provided by Esri, dating back to February 20, 2014. This application includes the World Imagery basemap, which is hosted in the ArcGIS Living Atlas [17].

2.1.2 Sentinel- 2 on Google Earth Engine

Sentinel-2 is a multispectral imaging mission developed by the European Space Agency (ESA) as part of the Copernicus Programme, designed for global land monitoring with high spatial, spectral, and temporal resolution [18]. The mission consists of two identical satellites, Sentinel-2A and Sentinel-2B, which together provide a 5-day revisit time at the equator. Each satellite carries the MultiSpectral Instrument (MSI), capturing 13 spectral bands ranging from the visible to shortwave infrared (443–2,190 nm), with spatial resolutions of 10 m, 20 m, or 60 m depending on the band. Sentinel-2 data is particularly valuable for applications in land cover classification, vegetation and water monitoring (e.g., NDVI and NDWI), agriculture, forest management, and disaster response due to its combination of high resolution and frequent revisit cycle. The data is freely available and pre-processed to Level-1C (top-of-atmosphere reflectance) and Level-2A (bottom-of-atmosphere surface reflectance) formats. On the Google Earth Engine (GEE) platform, Sentinel-2 data is available as part of its public data catalogue, enabling global-scale, cloud-based geospatial analysis. GEE hosts both Level-1C and Level-2A datasets:

- COPERNICUS/S2: Level-1C data (top-of-atmosphere reflectance)
- COPERNICUS/S2_SR: Level-2A data (surface reflectance) processed using Sen2Cor

The data is accessible through GEE's JavaScript and Python APIs, supporting rapid, scalable analyses with built-in tools for filtering by date, cloud cover, geometry, and band combinations. GEE also facilitates spectral index computation, image mosaicking, and time series analysis, making it a powerful platform for leveraging Sentinel-2's capabilities.

The GeoHAS channel change tool uses Sentinel-2 data to analyze annual changes on river crossings. For this study, we processed Sentinel 2 imagery between 2019 and 2024.

2.2 Study area

For this study, we selected three geographic areas in Peru based on their differences in fluvial dynamics (FIGURE 1). Two of these areas lie along the Pacific coast, specifically in the delta of two major rivers: the Tumbes River Basin and the Santa River Basin. In these areas, intense rainfall during ENSO (El Niño–Southern Oscillation) periods often triggers floods, causing significant inundations. The third area is in the Amazon region, in the Huallaga River basin. The Amazonian rivers exhibit significant seasonal fluctuations due to the rainfall patterns in the Andes. At this location within the Huallaga River basin, the terrain is characterized by flat slopes and broad alluvial plains promoting the formation of wide and dynamic rivers. These

rivers frequently shift their meandering paths, creating oxbow lakes [16].

AREA 1: Peruvian coast: Tumbes

Tumbes floodplain exhibits a mix of alluvial fluvial deposits composed of unconsolidated sediments transported and deposited by the Tumbes River. At the channel reaches the Tumbes River displays a meandering channel morphology with high sinuosity and permanent regime. The low longitudinal slope favors sediment accumulation and lateral channel mobility.

AREA 2: Peruvian coast

The area is made of recent alluvial deposits consisting of unconsolidated fluvial sediments. The Santa River displays an anastomosing morphology, characterized by multiple interconnected branches flowing through low-gradient terrain. This configuration promotes lateral instability.

AREA 3: Amazonian coast

Area 3 is located on a section of the Huallaga River, the longest tributary to the Maranon River flowing from Peruvian Cordillera Central [19]. The area is composed of unconsolidated sediments transported and deposited by the Huallaga River. At this section, the river exhibits a meandering channel morphology, with high sinuosity and evidence of lateral migration.

2.3 Time series monitoring

We employed Python algorithms to extract the annual active channel planform by integrating the Modified Normalized Difference Water Index (MNDWI) and the Normalized Difference Built-up Index (NDBI) (FIGURE 2). The Modified MNDWI is calculated as (Green - SWIR1)/ (Green + SWIR1) and enhances water features while suppressing built-up areas and vegetation noise that can interfere with standard NDWI calculations [20]. This analysis utilized cloud-free Sentinel-2 mosaics obtained from Google Earth Engine (GEE) from imagery collected between 2019 and 2024. The use of time series monitoring with Sentinel-2's systematic revisit cycle provides temporal continuity that addresses the inherent limitations of single-date high-resolution imagery acquisitions. The temporal resolution of Sentinel-2 allows the detection of seasonal channel migration patterns, flood-induced morphological changes, and gradual planform evolution that would otherwise remain unobserved in temporally sparse high-resolution datasets.

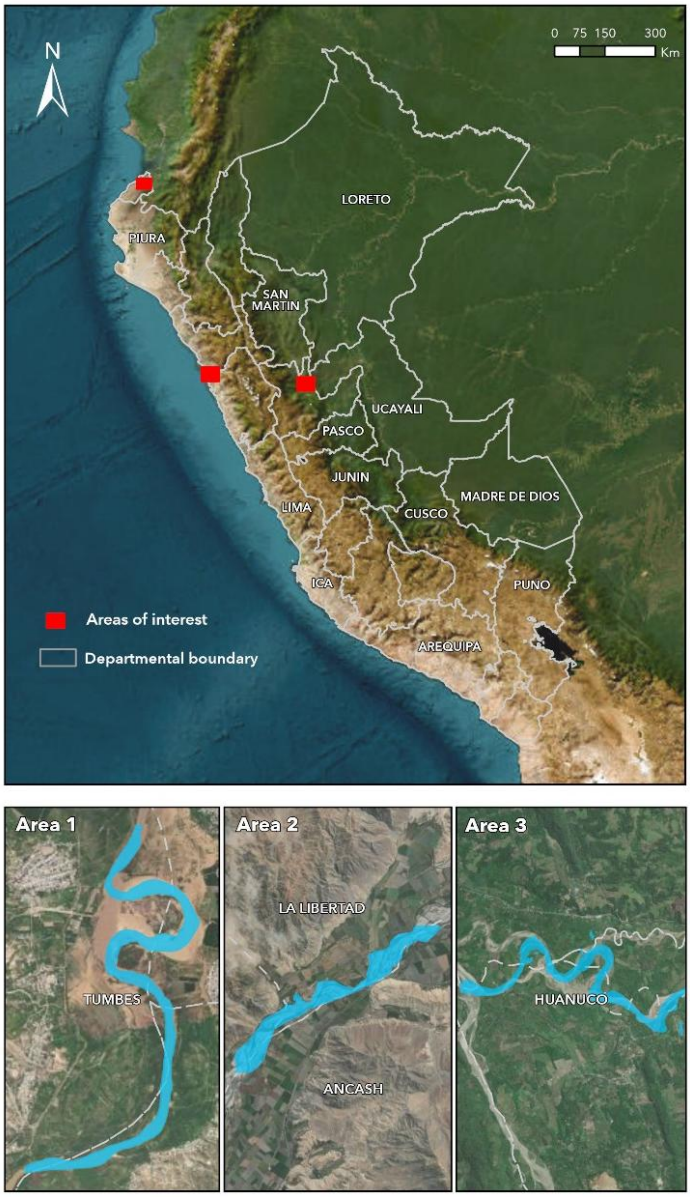

FIGURE 1: LOCATION OF THE STUDY AREAS (COAST AND AMAZON IN PERU)

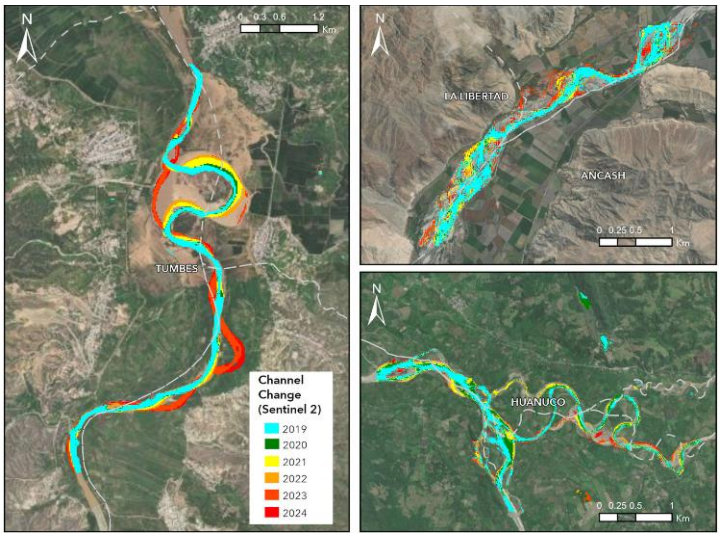

FIGURE 2: YEARLY CHANNEL CHANGES FOR AREAS 1 (LEFT), 2 (RIGTH-UP) AND 3 (RIGHT-BOTTOM) USING SENTINEL 2 DATA IN GEOHAS

2.4 Automated channel mapping

GeoHAS channel mapping module employs the samgeo [12, 21] based on the Segment Anything Model (SAM2-hiera-large) in Python for automated channel boundary extraction from high-resolution satellite and aerial imagery. Unlike traditional pixel-based classification approaches, samgeo provides object-aware segmentation that delineates complex channel geometries without requiring extensive training datasets specific to fluvial environments. Point-based detection demonstrates superior performance for channel mapping applications, requiring minimal user input while maintaining high accuracy in boundary delineation and reducing time. We iterated three times to map the channels in each area using the high-resolution satellite and aerial orthoimages provided by Esri. For Area 1, we mapped three periods (2018, 2021 and 2024). For Areas 2 and 3, only two years were deemed suitable for channel mapping.

2.5 Rate of change

To estimate the rate of change between the automated mapped channels, we followed a systematic approach. First, we established a reference grid over the study area. This grid consisted of an orthogonal line network aligned with the cardinal directions, creating intersecting frameworks that enabled standardized measurements of channel displacement across the reach.

Next, we computed the intersections between the channel boundaries and the grid for each temporal dataset, generating point networks that captured boundary positions at regular spatial intervals. These intersection points served as measurement nodes for quantifying positional changes between different periods, allowing for spatially explicit change detection.

Finally, our analysis included a change statistics analysis to determine annual erosion and accretion rates, as well as the maximum and mean boundary displacements along orthogonal axes and variations in channel width. All measurements were normalized to annual rates to facilitate comparisons across different temporal intervals and study periods.

2.6 Risk index

To evaluate the risk at infrastructure water crossing locations, we employed a composite weighted index that considers several factors: the rate of change within the channel reach, the trend of change (whether it is gradual or sudden), the maximum erosion at the crossing, and the ratio of channel width to the distance from the channel bank to the element at risk (used as a proxy for element at risk exposure). For infrastructure adjacent to meandering rivers, which face an encroachment threat, we only calculate the distance. In the case of buried infrastructure at the water crossing, the index also includes the average depth of cover to assess the potential exposure resulting from channel migration. The results of the analysis are reported on a structured report in the GeoHAS platform as a Level Two assessment (Level Two in the GeoHAS framework refers to detailed site evaluations to understand threat mechanisms and processes).

For standard water crossings:

$$RI = w_1 \times (\Delta C/\Delta t) + w^2 \times T + w4 \times E\_max + w4 \times (W/D\_inf)$$

For infrastructure adjacent to meandering rivers:

$$RI = w_1 \times (\Delta C/\Delta t) + w_2 \times T + w_3 \times E\_max + w_4 \times (1/D\_inf)$$

For buried infrastructure at water crossings:

$$RI = w_1 \times (\Delta C/\Delta t) + w_2 \times T + w_3 \times E\_max + w_4 \times (W/D\_inf) + w_5 \times (1/D\_cover)$$

Variable Definitions:

- RI = Risk Index (dimensionless)
- $(\Delta C/\Delta t)$ = Rate of channel change within the reach (m/year or m/time)
- T = Trend factor (dimensionless parameter quantifying gradual vs. sudden change patterns)
- E_max = Maximum erosion at the crossing location (m)
- W = Channel width (m)
- D_inf = Distance from infrastructure to element at risk (m)
- D_cover = Average depth of cover for buried infrastructure (m)
- w_1, w_2, w_3, w_4, w_5 = Weighting coefficients (dimensionless, $\Sigma w_i = 1$)

Notes:

- The (W/D_inf) ratio serves as a proxy for element-at-risk exposure
- For meandering river scenarios, encroachment threat is assessed using (1/D_inf) only
- The (1/D_cover) term for buried infrastructure accounts for potential exposure from channel migration

- Weighting coefficients should be calibrated based on local conditions, historical data, and expert judgment
- Higher RI values indicate greater risk to infrastructure integrity
- The RI results are then scaled to a 1 to 5 to make it consistent with GeoHAS scoring system

The index provides a quantitative framework for Level Two assessments in the GeoHAS platform, enabling systematic comparison and prioritization of infrastructure water crossing risks.

2.7 Limitations

Current limitations include:

(1) Variability in water levels across seasons, which can affect channel delineation and data availability. Future development will integrate hydrological data—such as precipitation and stream discharge records—to better contextualize observed planform changes and understand the geomorphic work associated with different flow regimes.

(2) The spatial resolution of Sentinel-2 images limits the examination of river dynamics to those rivers with a width of ten meters or more. Time series analysis of smaller rivers will likely require more frequent high-resolution data acquisition.

(3) Desktop analysis might limit the coefficients estimation in absence of field data.

3. RESULTS AND DISCUSSION

Figures 3 to 5, along with Table 1 below, present the multi-year channel map and the statistics obtained from our automated approach. In this section, we will discuss the results of the assessment, the insights we gained, and the improvements planned for our module development roadmap.

3.1 Channel mapping

Figure 3-5 illustrates the channel planform as mapped using high-resolution imagery obtained from ESRI Wayback. In each case, the automated module successfully identified the active channel for the analyzed periods. The point-based segmentation method allowed the user not only to map the channel planform but also identify channel bars, providing insights on how these river forms interact at the section.

At Area 1, we observed that the river exhibits an active fluvial dynamic, dominated by lateral migration processes. The multitemporal analysis revealed abrupt changes between 2023 and 2024, indicating a highly active system influenced by bank erosion and channel migration—typical characteristics of high-sinuosity rivers in alluvial plains.

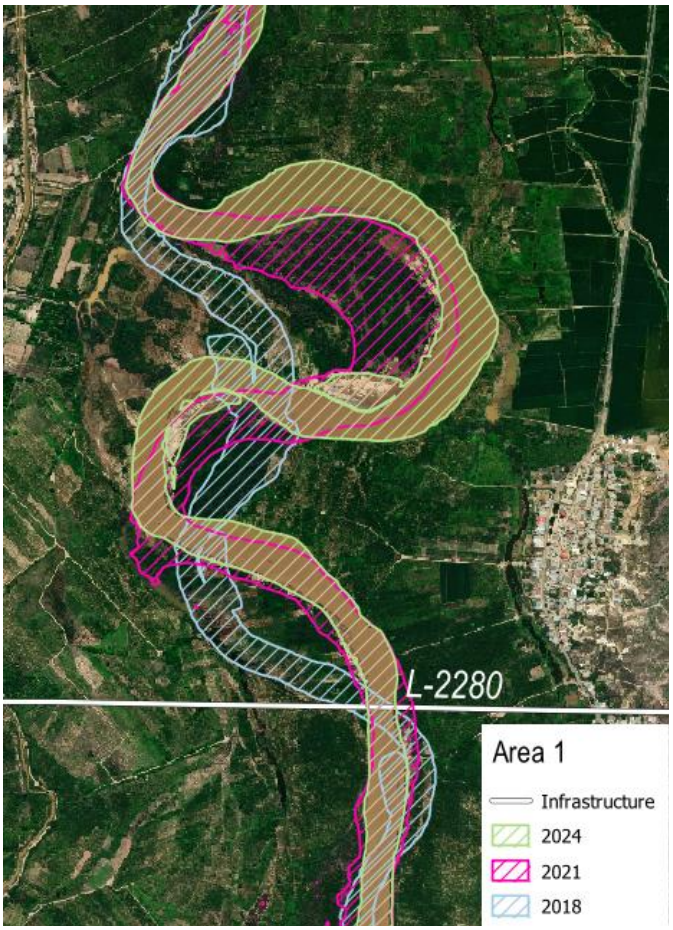

FIGURE 3: CHANNEL CHANGE MAPPING IN AREA 1.

At Area 2, most of the observed changes in the period occur within the active floodplain, with significant bank erosion occurring at the outside area of meander bends consistent with anastomosing morphologies.

FIGURE 4: CHANNEL CHANGE MAPPING IN AREA 2.

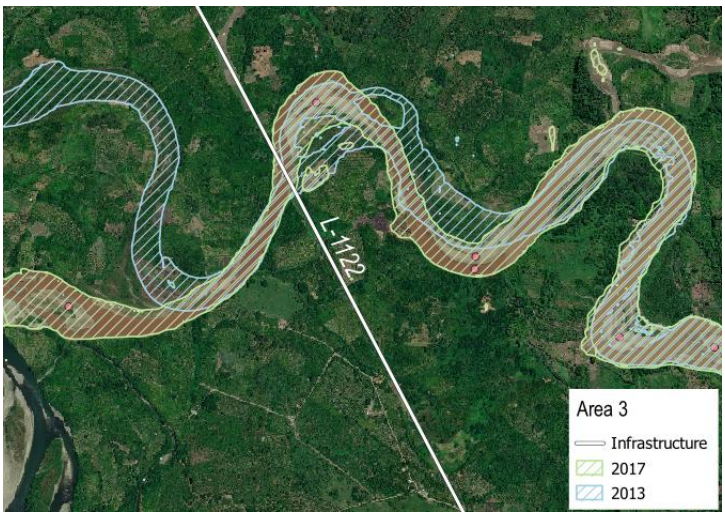

FIGURE 5: CHANNEL CHANGE MAPPING IN AREA 3.

At Area 3, the multitemporal analysis indicates that changes have been sudden, reflecting an active dynamic typical of sinuous rivers in alluvial plains.

3.2 Rate of change summary

Table 1 below shows the rate of change statistics obtained through the automated channel mapping exercise. For illustration purposes, this summary displays the results for all the study areas and does not discriminate between channel reaches. GeoHAS estimates the rate of change based on the channel reaches set up by the user. The risk index calculation uses the rate of change at the channel reach where the pipeline sits.

TABLE 1: SUMMARY OF THE RATE OF CHANGE FOR ALL THE AREAS

Year	Area 1		Area 2	Area 3
	2018-2021	2021-2024	2013-2019	2013-2017
Average displacement per year in axis Y (m)	54.1	53.4	-7.5	-47.4
Average displacement per year in axis X (m)	34.0	4.6	-22.4	80.6
Mean erosion in Y per year (m)	28.9	20.7	18.6	12.1
Mean erosion in X per year (m)	35.3	452.4	29.0	11.3
Max erosion in Y per year (m)	476.7	212.3	435.8	164
Max erosion in X per year (m)	474.0	452.4	355.0	216.9
Net erosion area (km^2)	0.3	0.1	0.1	0.1
Net accretion area (km^2)	1.6	0.2	0.1	0.1

Note: These results were consistent with a manual exercise we completed for all the study areas. Units: m= meters; km^2= square kilometers. Positive and negative numbers if the displacement value indicates the direction of the movement. Negative values in X-axis indicate movement to the west. Negative values in Y-axis indicate movement to the south.

From the statistics, we observe that Area 1 shows the most dynamic system with significant accretion (1.6 km² in 2018-2021) outweighing erosion, suggesting active channel meandering. Areas 2 and 3 show more balanced erosion/accretion ratios for the period, indicating more stable channel adjustment.

In summary, Area 1 experience active channel migration with significant sediment redistribution, while Areas 2 and 3 represent more constrained systems during the period. Based on the location of the evaluated infrastructure all these locations scored a very high risk.

3.3 Discussion and final thoughts

The temporal integration approach, using Sentinel-2, data is particularly valuable for capturing the full spectrum of channel activity across varying hydrological conditions at a river crossing, providing a more comprehensive understanding of long-term planform dynamics than would be achievable through intermittent high-resolution monitoring alone.

The SAM-based segmentation approach significantly reduces manual digitization requirements while maintaining boundary accuracy comparable to expert-generated channel maps. We repeated the exercise manually, and the automated process improved efficiency by a factor of 40.

The standardized grid analysis framework enables consistent change detection across diverse channel types and scales. Unlike reach-averaged approaches, the grid-based methodology preserves spatial variability in change patterns, enabling identification of localized erosion hotspots and preferential migration zones critical for process understanding and management applications.

The coupled methodology effectively captured gradual and sudden changes in channel planform triggered by seasonal variability and extreme weather events. Importantly, our results demonstrate the potential of high-resolution imagery to reliably monitor geomorphic changes at a resolution suitable for early warning and asset management. Future developments will include:

(1) including a hydrologic analysis of the watershed area that drains to the water crossing to extract correlations between water levels and imagery acquisition.

(2) centerline displacement in the time series analysis.

(3) expansion of time-series based on data from other sensors.

4. CONCLUSION

The findings reveal that river crossings with meandering and anastomosing morphology undergo average lateral displacements of tens of meters per year in wide and flat floodplains, with Area 1 showing the most pronounced changes in the analyzed period. These quantitative metrics feed directly into a weighted risk index, enabling operators to prioritize inspections, maintenance, and emergency preparedness at high-consequence locations. Because the approach benefits from freely available data and cloud-based processing, it is accessible to organizations with limited resources. High-resolution satellite imagery through platforms like SkyFy makes new acquisitions financially accessible.

We also note important limitations. Sentinel-2's 10 m resolution restricts analysis to channels wider than about ten meters, and seasonal water-level variability can complicate channel delineation. Further development should therefore integrate hydrological data (e.g., discharge records) to contextualize observed changes, incorporate centerline displacement metrics and explore the use of higher-resolution imagery for smaller rivers. Despite these challenges, the study underscores the value of remote sensing and AI as proactive tools for pipeline risk management in a changing climate and provides a foundation for future research into fully automated, real-time geohazard monitoring.

ACKNOWLEDGEMENTS

The authors would like to acknowledge that Daniel Cuervo developed the Python code in discussion with the main author. Also, that Luis Bastidas participated in early conversations of the ideas presented here.

REFERENCES

[1] Lagasse, P. F., Zevenbergen, L. W., Spitz, W. J., and Muter, B. A., 2004, Handbook for Predicting Stream Meander Migration, Transportation Research Board, Washington, D.C.

[2] Simon, A., and Rinaldi, M., 2006, "Disturbance, Stream Incision, and Channel Evolution: The Roles of Excess Transport Capacity and Boundary Materials in Controlling Channel Response," Geomorphology, 79(3–4), pp. 361–383.

[3] Bracic, J. J., Malcovish, C., and Yaremko, E., 2014, "Risk Management for Lateral Channel Movement at Pipeline Water Crossings," Proc. 10th Int. Pipeline Conf. (IPC 2014), Calgary, Alberta, Canada, Sept. 29–Oct. 3, Paper No. IPC2014 33632.

[4] Avendaño, J. A., and García López, M., 2013, "Analysis of Undermining and Lateral Erosion to Maximize Designs of River Crossing of Pipelines," Proc. ASME 2013 Int. Pipeline Geotechnical Conf. (IPG 2013), Bogotá, Colombia, July 24–26, Paper No. IPG2013 1914.

[5] Larsen, E. W., Premier, A. K., and Greco, S. E., 2006, "Cumulative Effective Stream Power and Bank Erosion on the Sacramento River, California, USA," J. Am. Water Resour. Assoc., 42(4), pp. 1077–1097.

[6] Manfreda, S., Miglino, D., Saddi, K. C., Jomaa, S., Eltner, A., and Perks, M., 2024, "Advancing River Monitoring Using Image Based Techniques: Challenges and Opportunities," Hydrological Processes, 38(5), pp. 657–677.

[7] Chandler, J., Ashmore, P., Paola, C., Gooch, M., and Varkaris, F., 2002, "Monitoring River Channel Change Using Terrestrial Oblique Digital Imagery and Automated Digital Photogrammetry," Annals of the Association of American Geographers, 92(4), pp. 631–644.

[8] Lane, S. N., James, T. D., and Crowell, M. D., 2003, "Application of Digital Photogrammetry to Complex Topography for Geomorphological Research," The Photogrammetric Record, 16(95), pp. 793–821.

[9] Westoby, M. J., Brasington, J., Glasser, N. F., Hambrey, M. J., and Reynolds, J. M., 2012, "Structure from Motion Photogrammetry: A Low Cost, Effective Tool for Geoscience Applications," Geomorphology, 179, pp. 300–314.

[10] Rinaldi, M., 2023, Le Applicazioni della Dinamica Fluviale alla Gestione dei Corsi d'Acqua, Università degli Studi di Firenze, Firenze, Italy.

[11] Carrivick, J. L., and Smith, M. W., 2018, "Fluvial and Aquatic Applications of Structure from Motion Photogrammetry and Unmanned Aerial Vehicle/Drone Technology," Wiley Interdisciplinary Reviews: Water, 5(1), e1252.

[12] Wu, Q., and Prado Osco, L., 2023, "samgeo: A Python Package for Segmenting Geospatial Data with the Segment Anything Model (SAM)," Journal of Open Source Software, 8(93), 5663.

[13] Rakhal, B., Adhikari, T., Sharma, S., and Ghimire, G., 2021, "Assessment of Channel Shifting of Karnali Megafan in Nepal Using Remote Sensing and GIS," Annals of GIS, DOI: 10.1080/19475683.2021.1871950.

[14] Ibn Sultan, R., Li, C., Zhu, H., Khanduri, P., Brocanelli, M., and Zhu, D., 2023, "GeoSAM: Fine Tuning SAM With Multimodal Prompts for Mobility Infrastructure Segmentation," arXiv preprint, arXiv:2311.11319.

[15] Valverde, H., Abad, J. D., Guerrero, L., and Estrada Terrel, Y. R., 2024, "Hydrogeomorphic Characterization of the

Huallaga River for the Peruvian Amazon Waterway," Journal of Waterway, Port, Coastal, and Ocean Engineering, 150(2).

[16] Guerrero, L., Abad, J. D., Ortals, C., Valderde, H., Estrada, Y., Chicchon, H., et al., 2024, "Hydrogeomorphology of the Origin of the Amazon River: The Confluence Between the Marañón and Ucayali Rivers," Earth Surface Processes and Landforms, 49(12), pp. 3949–3967.

[17] Mamini, J., 2022, "World Imagery Wayback – 2025 Enhancements," ArcGIS Blog, Esri, accessed July 25 2025, at https://www.esri.com/arcgis-blog/products/arcgis-living-atlas/imagery/world-imagery-wayback-2025-updates.

[18] Drusch, M., Del Bello, U., Carlier, S., Colin, O., Fernandez, V., Gascon, F., et al., 2012, "Sentinel 2: ESA's Optical High Resolution Mission for GMES Operational Services," Remote Sensing of Environment, 120, pp. 25–36.

[19] Naito, K., Valverde, H., Estrada, Y., Guerrero, L., Canas, C., and Abad, J. D., 2019, "Geomorphological Characteristics of the Huallaga River, Peru," AGU Fall Meeting Abstracts, EP51E 2137.

[20] Xu, H., 2006, "Modification of Normalised Difference Water Index (NDWI) to Enhance Open Water Features in Remotely Sensed Imagery," International Journal of Remote Sensing, 27(14), pp. 3025–3033.

[21] Osco, L. P., Wu, Q., de Lemos, E. L., Gonçalves, W. N., Ramos, A. P. M., Li, J., and Junior, J. M., 2023, "The Segment Anything Model (SAM) for Remote Sensing Applications: From Zero to One Shot," International Journal of Applied Earth Observation and Geoinformation, 124, 103540.Abad, J. D., Garcia, A. P., Marín-Díaz, J., Escobar, C., Ortals, C., & Chicchon, H. (2025). Morphodynamics of anabranching structures in the Peruvian Amazon River. Earth Surface Processes and Landforms, 50(1), e6020.